Clays and Clay Minerals, Vol. 57, No. 3, 353–360, 2009.

FACTORS GOVERNING THE FORMATION OF LITHIOPHORITE AT ATMOSPHERIC PRESSURE

HAOJIE CUI[1,2], LEI YOU[1], XIONGHAN FENG[1,*], WENFENG TAN[1], GUOHONG QIU[1], AND FAN LIU[1]

[1] Key Laboratory of Subtropical Agricultural Resources and Environment, Ministry of Agriculture, Huazhong Agricultural University, Wuhan 430070, China

[2] Institute of Urban Environment, Chinese Academy of Science, Xiamen 361021, China

Abstract—Lithiophorite is a naturally occurring Mn oxide mineral commonly found in soils and sediments. The usual method of synthesizing lithiophorite is *via* a hydrothermal process in an autoclave at relatively high temperature and pressure. In the present study, an alternative, reflux method, at atmospheric pressure, for synthesis of lithiophorite was developed successfully. The influence of reaction duration, temperature, type of precursor birnessite (H-birnessite, Na-birnessite, aged Na-birnessite), and pH on the formation of lithiophorite were investigated by reflux treatment of lithium-aluminum hydroxide complex ion ($Li_xAl_n(OH)_m^{z+}$)-exchanged birnessite. The results show that the degree of conversion of lithiophorite decreases with decreasing reaction temperature. Lithiophorite can be obtained at pH values from 5.0 to 9.0, but a circumneutral pH is more favorable for formation at atmospheric pressure. Conversion of Na-birnessite (Bir-OH) to lithiophorite is more favored than aged Na-birnessite (Bir-OH-A). Lithiophorite was not obtained by refluxing the $Li_xAl_n(OH)_m^{z+}$ ion-exchanged H-birnessite (Bir-H) sample. The rate of conversion of lithiophorite increases with increasing reflux time. Lithiophorite synthesized by a reflux process has pseudo-hexagonal crystals of 0.1–0.5 μm with a chemical composition of $Li_{0.24}Al_{0.46}MnO_{2.67}(H_2O)_{1.25}$. The results have important implications for the origin and underlying mechanism of lithiophorite formation in the environment.

Key Words—Birnessite, Lithiophorite, Manganese Oxide, Refluxing.

INTRODUCTION

Manganese oxide minerals are ubiquitous in soils and sediments and participate in a wide variety of chemical reactions, such as oxidation-reduction and cation-exchange reactions, which affect the compositions and chemical behaviors of sediments, soils, and associated aqueous systems (Post, 1999). Lithiophorite is a naturally occurring Mn oxide mineral with a sandwich layered structure, consisting of MnO_6 octahedral sheets alternating with sheets of $LiAl_2(OH)_6$ octahedra (Post and Appleman, 1994; Feng *et al*., 1998, 1999; Yang and Wang, 2003). Natural lithiophorites typically occur as poorly crystalline nm-sized particles or as coatings coexisting with other minerals such as other Mn oxides, Fe oxides, and clay minerals (Uzochukwu and Dixon, 1986; Golden *et al*., 1993; Tan *et al.*, 2006; Ouvrard *et al*., 2005; Dowding and Fey, 2007). Lithiophorite is commonly found in weathered zones of Mn deposits and in certain acid soils (De Villiers, 1983). The occurrence of lithiophorite in acid soils suggests that it is formed by alteration of birnessite (Mckenzie, 1989). The formation of lithiophorite requires a relatively large concentration of Al^{3+} (Golden *et al*., 1993). As one of the major Mn minerals in soils and sediments, lithiophorite can be viewed as a scavenger of metals in soils since they enhance the stability of the layered double oxyhydroxide phase (Manceau *et al*., 2004). For example, As(V) was found to be sorbed on lithiophorite-type particles through surface-complexation type reactions (Ouvrard *et al*., 2005).

Due to the relatively small amount and poor crystallinity of lithiophorite in soils, it is not easily separated for study. Synthesis of lithiophorite, therefore, is the best means by which to study its structures, formation, and reactivity. Wadsley (1950) synthesized lithiophorite by substitution of Al and Li into Na-buserite, followed by hydrothermal treatment of the product. Giovanoli *et al*. (1973) prepared a similar material by hydrothermal treatment of birnessite with Al and Li hydroxides. Another hydrothermal chemical process for synthesis of lithiophorite from $Li_xAl_n(OH)_m^{z+}$ ion-exchanged birnessite was proposed by Feng *et al*. (1998, 1999). During synthesis, impurities such as γ-AlOOH or other unidentified compounds were found in the products. More recently, a pure lithiophorite was prepared successfully by hydrothermal treatment of a mixture of birnessite, $NaAl(OH)_4$, and $LiOH{\cdot}H_2O$ under highly alkaline conditions (Yang and Wang, 2003). Their results show that Li^+, Al^{3+}, and hydrothermal treatment are all necessary for the formation of lithiophorite.

Many studies have reported that lithiophorite can be synthesized under hydrothermal conditions in an auto-

* E-mail address of corresponding author:
fxh73@mail.hzau.edu.cn
DOI: 10.1346/CCMN.2009.0570307

clave at relatively high temperature and pressure, but the formation of lithiophorite at Earth-surface conditions is not well documented and the mechanism is not fully understood. Study of the formation of lithiophorite at atmospheric pressure and under other known conditions is important in our understanding of the origins of lithiophorite in the environment. In the present study, the synthesis of lithiophorite by a reflux method at atmospheric pressure and under other conditions such as the type of precursor birnessite, the reaction temperature and duration, and the pH was investigated.

MATERIALS AND METHODS

Preparation of H-birnessite

H-birnessite (Bir-H) was synthesized using a modified version of the procedure of Mckenzie (1971): 500 mL of 0.4 mol/L $KMnO_4$ was heated, kept boiling in an oil bath, and stirred continuously. A solution of 35 mL of concentrated HCl (12 mol/L) and 15 mL of DDW (distilled, deionized water, 18 MΩ, from Labconco Water Pro Ps, used throughout the experiments) was added dropwise to the $KMnO_4$ solution at a rate of 0.7 L/min. After reacting under boiling, for a further 30 min, the mixture solution was cooled, aged for 12 h at 60ºC, and centrifuged at 2.54×10^{-4} g in a Beckman Super-speed refrigerated centrifuge. The mineral was washed with DDW until no Cl^- was detected by a 0.1 mol/L acidic silver nitrate solution (Feng *et al*., 2007). The Bir-H sample has the chemical composition of $K_{0.05}MnO_{2.01}{\cdot}xH_2O$.

Preparation of Na-birnessite

Na-birnessite (Bir-OH) was synthesized as follows (Feng *et al*., 2004): 250 mL of 5.5 mol/L NaOH solution (<0ºC) was added quickly to 200 mL of 0.5 mol/L $MnCl_2$ solution to form a white $Mn(OH)_2$ precipitate, and O_2 was bubbled through it immediately at a rate of 1.5 L/min. After oxidation for 5 h, the black precipitate was washed with DDW until the pH was ~7. Some of the washed sample was aged in water for 90 days. The samples are designated Bir-OH and Bir-OH-A, respectively, and have the compositions $Na_{0.29}MnO_{1.98}{\cdot}xH_2O$ and $Na_{0.27}\ MnO_{1.98}{\cdot}xH_2O$, respectively.

Preparation of lithium-aluminum hydroxide complex ions

A solution of lithium-aluminum hydroxide complex ions ($Li_xAl_n(OH)_m^{z+}$) was prepared by slowly adding dropwise a solution of 0.5 mol/L LiOH (400 mL) into a solution of 0.2 mol/L $Al(NO_3)_3$ (500 mL) (Li/Al mole ratio = 2.0) at 60ºC with stirring. The solution was aged at 60ºC for 2 h and filtered to remove precipitates (Feng *et al*., 1998). The concentrations of Li and Al were 0.222 mol/L and 0.072 mol/L, respectively. The Li/Al mole ratio of the $Li_xAl_n(OH)_m^{z+}$ complex ions solution was 3.08.

Ion-exchange of birnessites and conversion to lithiophorites

2 g of Bir-OH was dispersed in 300 mL of $Li_xAl_n(OH)_m^{z+}$ with mild stirring for 24 h to exchange $Li_xAl_n(OH)_m^{z+}$ complex ions for Na^+ ions in the interlayer space of Bir-OH. The ion-exchange treatment was repeated twice to complete the ion-exchange reaction. The ion-exchanged sample was washed with distilled water and dispersed in water to prepare the suspension. The pH values of the suspension were adjusted to 5.0, 7.0, and 9.0 using LiOH solution to identify the effects of pH on the formation of lithiophorite. These suspensions were transferred to flasks and refluxed (100ºC) with stirring for 5 days at atmospheric pressure. The refluxed solutions were centrifuged and the products were washed 3−5 times with DDW and dried.

The treatment of Bir-H and Bir-OH-A was similar to that of the Bir-OH sample but the pH was maintained at 7.0. Suspensions of the Bir-OH sample were heated at 100ºC, 60ºC, and 40ºC and samples of intermediate products taken in order to characterize the effects of temperature and reflux time on the formation of lithiophorites.

Chemical analysis

The chemical compositions of the Mn oxides and the elemental content of the solution of complex ions were analyzed using a Varian Vista-MPX ICP-OES (ICP). Approximately 100 mg of sample was dissolved in 50 mL of aqua regia and diluted to 1000 mL. The concentrations of Li, Na, Al, and Mn were analyzed at wavelengths of 610.365, 589.592, 273.312, and 257.610 nm, respectively. All chemical analyses were repeated three times and the mean values recorded.

X-ray diffraction (XRD) analysis

X-ray diffraction was carried out at ambient temperature, using a D/Max-3B diffractometer equipped with monochromated CuKα radiation (λ = 0.1541 nm) or FeKα radiation (λ = 0.1937 nm). The diffractometer was operated at a tube voltage of 40 kV, a current of 20 mA, and a step scanning rate of 0.02º/0.5 s.

Transmission electron microscopy (TEM) measurements

The samples were crushed gently to powder, dispersed in anhydrous ethanol, sonicated, deposited on a holey copper grid, and air dried. The TEM images and electron diffraction patterns were captured using a Philips-CM12 TEM at an accelerating voltage of 120 kV.

RESULTS AND DISCUSSION

Effects of pH

The XRD data illustrating the effects of variable pH on solid-phase transformation (Figure 1) revealed two strong diffraction peaks for lithiophorite at 0.95 nm

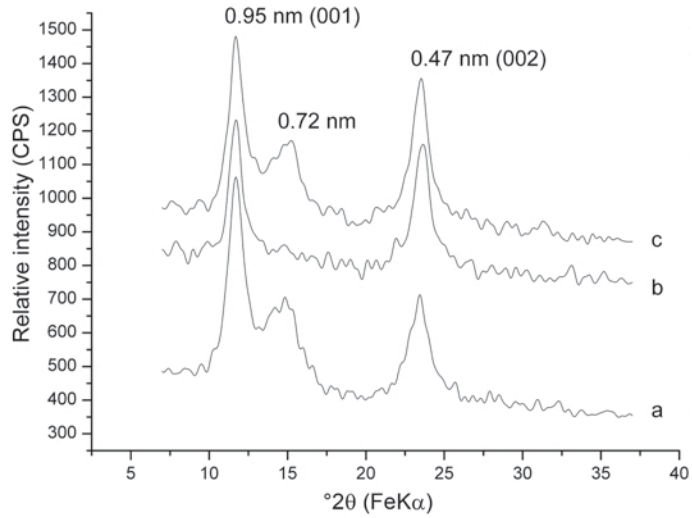

Figure 1. XRD patterns of the products of refluxing treatment of Bir-OH samples exchanged with lithium-aluminum hydroxide complex ions ($Li_xAl_n(OH)_m^{z+}$) at (a) pH 5.0, (b) pH 7.0; and (c) pH 9.0.

(001) and 0.47 nm (002) (Figure 1a) and a weak diffraction peak for birnessite at 0.72 nm, indicating that most of the birnessite was converted to lithiophorite. Only peaks characteristic of lithiophorite appeared in the XRD pattern of the refluxed product at pH 7.0, suggesting that all of the birnessite was converted to lithiophorite (Figure 1b). The peaks characteristic of lithiophorite and birnessite in the XRD pattern of the refluxed product at pH 9.0 are similar to those at pH 5.0, indicating that some of the birnessite was not converted to lithiophorite (Figure 1c), suggesting that the phase transformation from birnessite to lithiophorite was affected by the pH, and that lithiophorite could form over a relatively wide range of pH values from 5.0 to 9.0. This result is in accord with the occurrence of natural lithiophorites in acid and alkaline soils (Mckenzie, 1989; Tan *et al*., 2006).

The chemical compositions of products of $Li_xAl_n(OH)_m^{z+}$ ions exchanged with samples of Bir-OH at different pH are shown in Table 1. The Li content in the samples increased with increasing pH, and the Al and Mn contents remained constant indicating that the compositions of the $Li_xAl_n(OH)_m^{z+}$ ions may change with changes in the pH with a resultant effect on the phase transformation from birnessite to lithiophorite.

Table 1. Chemical compositions of products of $Li_xAl_n(OH)_m^{z+}$ ions exchanged with Bir-OH samples at different pHs.

pH	Li (mmol/g)	Al (mmol/g)	Mn (mmol/g)	Li/Al/Mn
5	0.84	3.62	7.09	1/4.31/8.44
7	1.85	3.50	6.96	1/1.89/3.76
9	2.68	3.48	7.07	1/1.30/2.64

Effects of the type of birnessites

The XRD patterns of the synthetic samples have peaks at *d* spacings of 0.72, 0.36, and 0.23 nm (Figure 2) which are characteristic of birnessite without impurities. As shown in Figure 2, the intensity of 0.72 nm diffraction peak decreases as follows: Bir-OH-A > Bir-OH > Bir-H, indicating that Bir-OH-A is the most crystalline and Bir-H is the least crystalline. Transmission electron microscopy images (Figure 3) of the synthetic birnessites show that Bir-H consists of clusters or ball-like aggregates, 0.5−1 μm in size (Figure 3a). The aggregates are randomly stacked, thin-plate structures, when observed under high magnification (Feng *et al*., 2007). The Bir-OH contains both needle- and plate-shaped crystallites. The plates are irregular in shape and 0.1−0.5 μm in size (Figure 3b). The Bir-OH-A plates are well-stacked, hexagonal plates, 0.5−2 μm in size (Figure 3c), suggesting that the crystallization of synthetic birnessite was further enhanced by the aging treatment. These results are in good agreement with the XRD analysis results.

The XRD patterns of the three ion-exchanged birnessites revealed only one layered phase with a basal spacing of 0.72 nm in the Bir-H sample (Figure 4a) and two layered phases with basal spacings of ~0.95 and 0.72 nm were observed in the Bir-OH and Bir-OH-A samples (Figure 4b,c). The 0.95 nm peak for Bir-OH was more intense than that of Bir-OH-A. The 0.95 nm basal spacing corresponds to a layered phase with $Li_xAl_n(OH)_m^{z+}$ complex ions between the sheets of the MnO_6 octahedra (Feng *et al*., 1999) suggesting that $Li_xAl_n(OH)_m^{z+}$ ions are most easily inserted into the interlayer space of the Bir-OH sample.

The elemental contents of the different synthetic birnessites and their intercalated compounds are given in Table 2. The intercalated compounds have similar Mn contents, but the Li and Al contents vary depending on

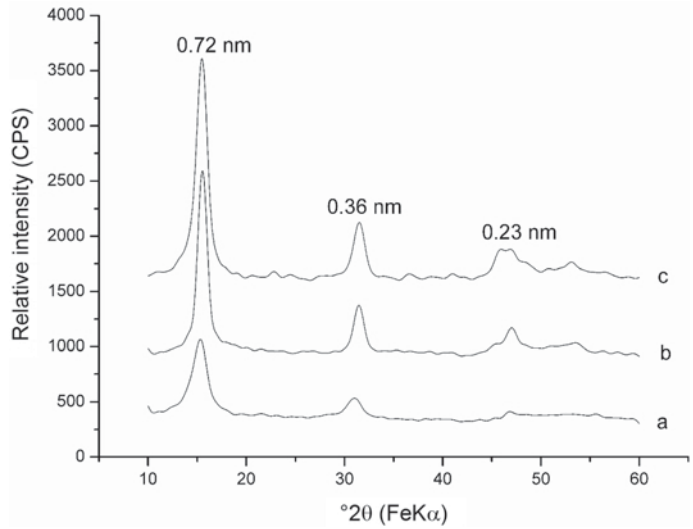

Figure 2. XRD patterns of synthetic birnessites prepared by different methods: (a) Bir-H, (b) Bir-OH, and (c) Bir-OH-A.

the type of birnessite. The exchanged Bir-OH and Bir-OH-A contain more Li and Al than the Bir-H sample, indicating that $Li_xAl_n(OH)_m^{z+}$ ions can more easily enter the interlayers of Bir-OH and Bir-OH-A than of Bir-H.

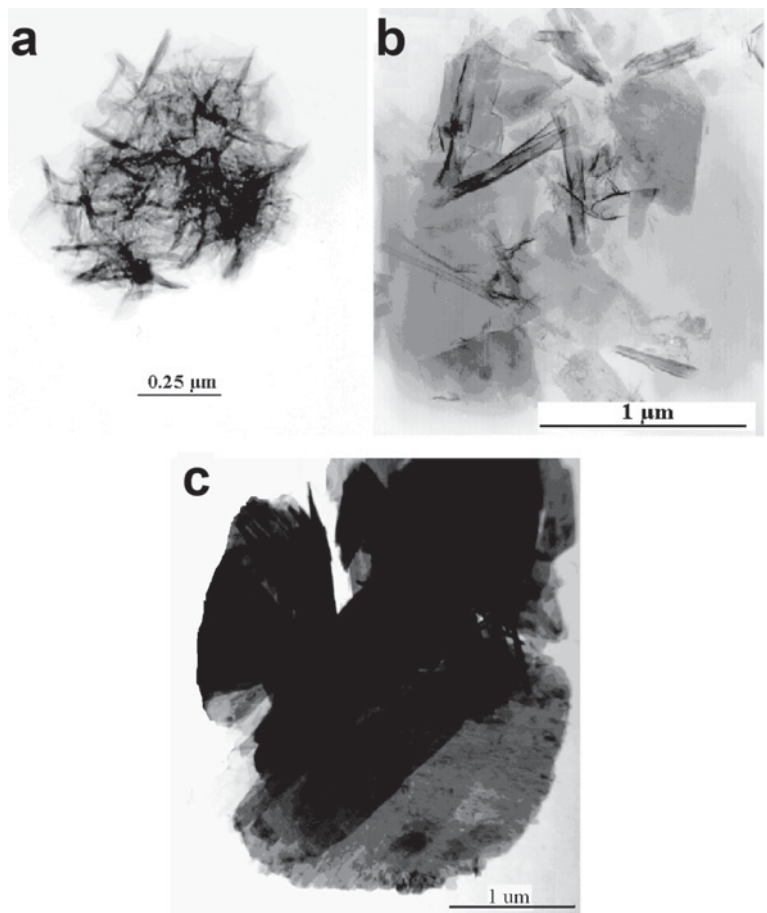

Figure 3. TEM images of synthetic birnessites prepared by different methods: (a) Bir-H, (b) Bir-OH, and (c) Bir-OH-A.

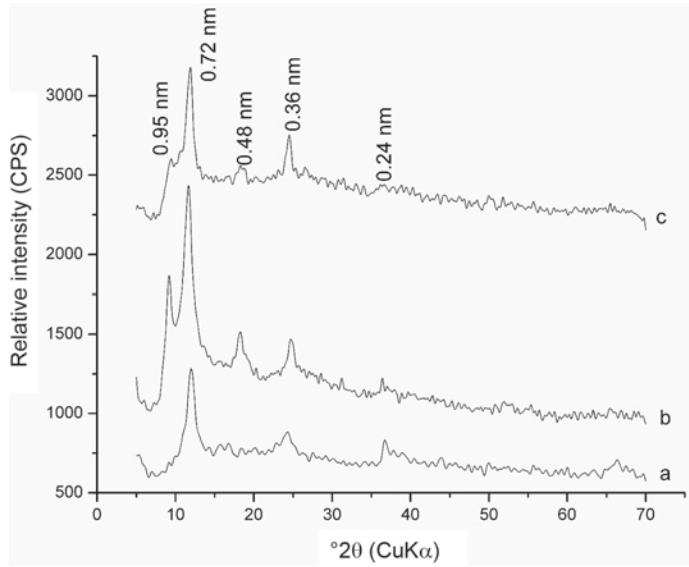

Figure 4. XRD patterns of three ion-exchange treated birnessites: (a) Bir-H, (b) Bir-OH, and (c) Bir-OH-A.

The effect of the method used to synthesize the precursor birnessites on the formation of lithiophorite was also studied. The XRD patterns of the reflux products obtained from the precursor birnessites, using the $Li_xAl_n(OH)_m^{z+}$-templating reaction, revealed that, for Bir-H, only the peaks of birnessite were present (Figure 5a), suggesting that the Bir-H sample had not been converted to lithiophorite. When Bir-OH was used for the synthesis, only strong diffraction peaks of lithiophorite at 0.95 nm (001) and 0.47 nm (002) were obtained (Figure 5b), indicating that all birnessite was converted to lithiophorite. For Bir-OH-A, strong diffraction peaks of lithiophorite and a weak peak of birnessite were obtained (Figure 5c), indicating that a small amount of birnessite remained unconverted.

Previous reports suggested that lithiophorite can form by alteration of birnessite with a relatively large Al^{3+} concentration (Mckenzie, 1989; Golden *et al*., 1993; Dowding and Fey, 2007). For the formation of lithiophorite by treatment of $Li_xAl_n(OH)_m^{z+}$ ion-exchanged birnessite, the $Li_xAl_n(OH)_m^{z+}$ ions should first be inserted into the interlayer of birnessite by an ion-exchange reaction (Feng *et al*., 1999). When the Bir-OH sample is used to prepare lithiophorite, the $Li_xAl_n(OH)_m^{z+}$ ions can easily enter the interlayer of birnessite by ion-exchanging with interlayer Na^+ cations, and lithiophorite can be obtained by reflux treatment of the mixed-layer phase of Mn oxide with basal spacings of 0.72 and 0.95 nm. However, the H^+ and K^+ cations in the interlayer of Bir-H sample are difficult to replace by $Li_xAl_n(OH)_m^{z+}$ ions and no lithiophorite is obtained after refluxing the ion-exchanged Bir-H sample. Lithiophorites contain a large proportion of Mn^{3+} in their structures (Kim *et al*., 2002; Yang and Wang, 2003; Manceau *et al*., 2005). Luo *et al*. (1999) reported that Mn^{3+} in Na-buserite may disproportionate into Mn^{4+} and Mn^{2+} during the aging process. The amount of Mn^{3+} in the structure of Bir-OH will thus decrease during the aging process, a possible reason for the decreased amount of lithiophorite formed from aged Bir-OH.

Effects of temperature

The XRD patterns of the products from heating $Li_xAl_n(OH)_m^{z+}$- exchanged Bir-OH at different temperatures were measured (Figure 6). When ion-exchanged samples were refluxed at 40ºC for 5 days, a weak

Table 2. Chemical analysis results of the different synthetic birnessites and their intercalated elements.

Sample	Na (mmol/g)	K (mmol/g)	Li (mmol/g)	Al (mmol/g)	Mn (mmol/g)	Li/Al/Mn
Bir-OH	2.94				8.79	
Bir-OH-A	2.83				8.75	
Bir-H		0.55			9.16	
Bir-OH-exchange			1.85	3.50	6.96	1/1.89/3.76
Bir-OH-A-exchange			1.78	3.20	6.47	1/1.80/3.63
Bir-H-exchange		0.41	0.92	0.75	6.65	1/0.82/7.23

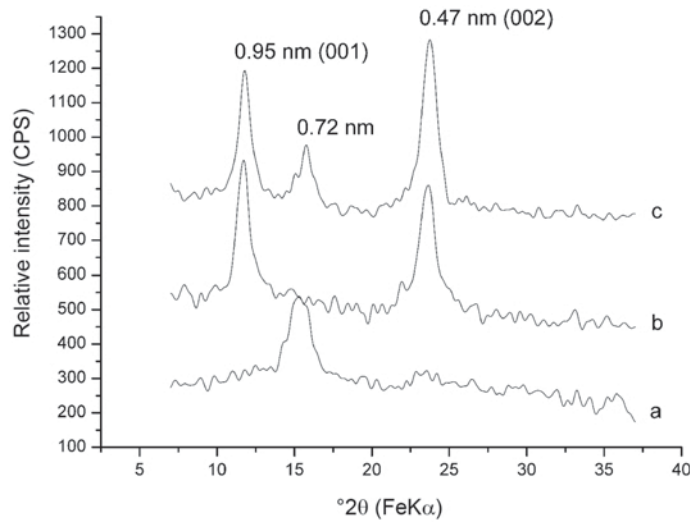

Figure 5. XRD patterns of the refluxed products of different birnessites exchanged with lithium-aluminum hydroxide complex ions ($Li_xAl_n(OH)_m^{z+}$). (a) Bir-H, (b) Bir-OH, and (c) Bir-OH-A.

diffraction peak of lithiophorite at 0.47 nm (002) and a strong diffraction peak of birnessite at 0.72 nm in the XRD pattern of products were observed, indicating that some of the birnessite was converted to lithiophorite (Figure 6a). When the temperature was increased to 60ºC, the intensity of the characteristic lithiophorite peaks increased and the intensity of the characteristic birnessite peak decreased, suggesting that more birnessite was converted to lithiophorite (Figure 6b). When the ion-exchanged sample was heated at 100ºC, the characteristic diffraction peaks of birnessite almost disappeared, and the characteristic diffraction peaks of lithiophorite at 0.95 nm (001) and 0.47 nm (002) became strong, indicating that birnessite was completely converted to lithiophorite (Figure 6c). The formation reaction of the sandwich layered structure of lithiophorite consisted of two steps: hydrolysis of $Li_xAl_n(OH)_m^{z+}$ and dehydration of crystal water from the interlayer space of the layered structure (Feng *et al*., 1999). The transformation reaction from the 0.95/0.72 nm mixed-layer phase to lithiophorite would be accelerated by the increase in treatment temperature.

Effects of refluxing time

The XRD patterns in Figure 7 show the phases of the intermediate products at the different stages of reflux treatment of complex ion-exchanged Bir-OH. A weak diffraction peak of lithiophorite at 0.95 nm (001) and a strong peak of birnessite at 0.72 nm in the XRD pattern of intermediates were obtained after 1 day of reflux,

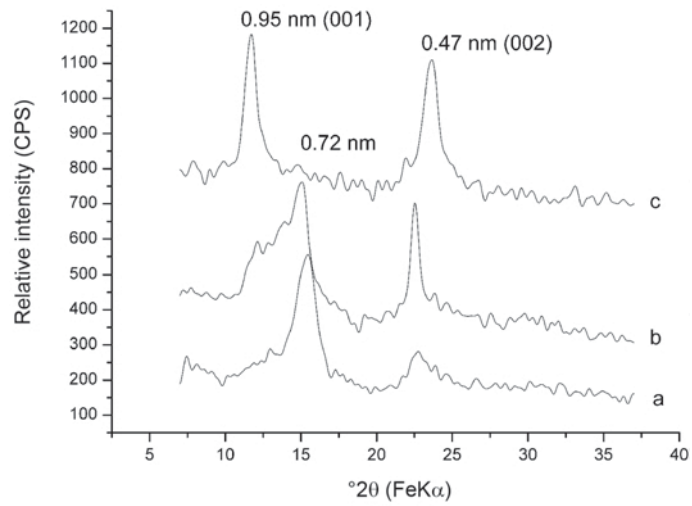

Figure 6. XRD patterns of the refluxed products of Bir-OH exchange with lithium-aluminum hydroxide complex ions ($Li_xAl_n(OH)_m^{z+}$) (a) heated at 40ºC, (b) heated at 60ºC, and (c) heated at 100ºC.

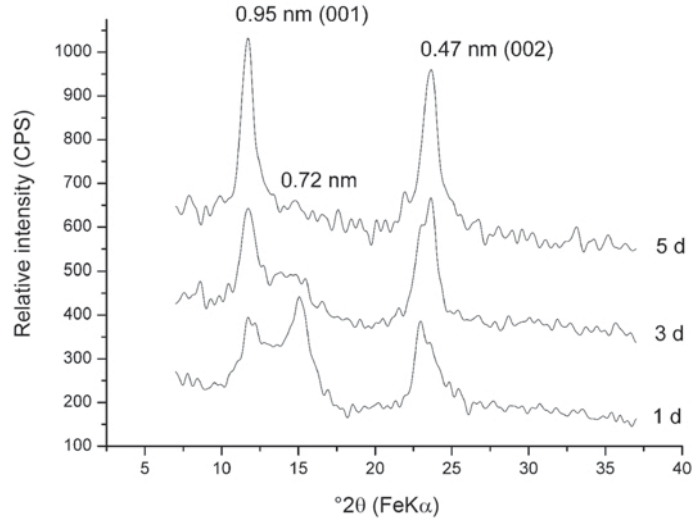

Figure 7. XRD patterns of intermediate products at different stages of reflux treatment of Bir-OH exchanged with lithium-aluminum hydroxide complex ions ($Li_xAl_n(OH)_m^{z+}$).

indicating that some birnessite was converted to lithiophorite. After 3 days of reflux (at 100ºC), the diffraction peak of birnessite almost disappeared, and the lithiophorite peak became strong, indicating that birnessite was largely converted to lithiophorite. When the reflux time was extended to 5 days, the characteristic peaks of birnessite disappeared, and the lithiophorite peaks became stronger, indicating that the crystallinty of the product was further enhanced.

The TEM image and electron diffraction (ED) pattern of the synthetic lithiophorite are shown in Figure 8. The ED pattern was well indexed based on a monoclinic-symmetry unit cell with parameters a = 0.506 nm, b = 0.291 nm, c = 0.955 nm, and 100.5º (JCPDS 16-364). Synthetic lithiophorite consists of small pseudo-hexagonal crystals 0.1−0.5 μm in size. The morphological characteristics of the synthetic lithiophorite are similar to those of the natural samples and to those synthesized hydrothermally by other researchers (Giovanoli *et al*., 1973; Golden *et al*., 1993; Vidhana Arachchi *et al*., 2004; Dowding and Fey, 2007). The average chemical composition of the lithiophorite synthesized by refluxing for 5 days at pH 7.0 was $Li_{0.24}Al_{0.46}MnO_{2.67}(H_2O)_{1.25}$. This is close to the ideal composition of lithiophorite with a Li:Al:Mn atomic ratio of 1:2:3 except for a slightly large Mn content.

CONCLUSIONS

Lithiophorite can be formed from synthetic birnessites and is affected by several reaction conditions at atmospheric pressure. The conversion rate to lithiophorite

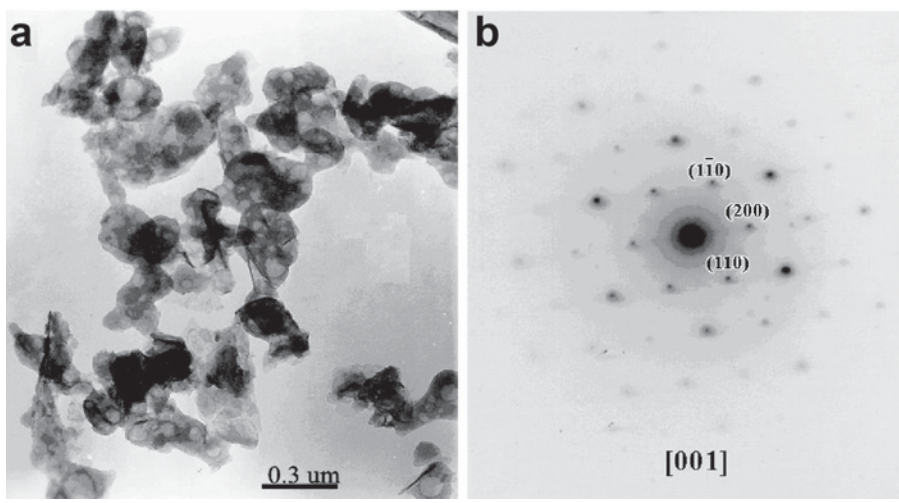

Figure 8. TEM image (a) and ED pattern (b) of the synthetic lithiophorite.

decreases with decreasing reaction temperature. Bir-OH is converted to lithiophorite more easily than aged Bir-OH, and no lithiophorite is obtained by refluxing Bir-H exchanged with the $Li_xAl_n(OH)_m^{z+}$ ion. The phase transformation from birnessite to lithiophorite is also affected by pH. Lithiophorite can be obtained at pH values from 5 to 9, but the rate of conversion to lithiophorite follows the sequence: neutrality > alkali ≈ acidic. The rate of conversion to lithiophorite is increased with prolonged reflux time. Synthetic lithiophorite consists of small pseudo-hexagonal crystals 0.1−0.5 μm in size, and the chemical composition is $Li_{0.24}Al_{0.46}MnO_{2.67}(H_2O)_{1.25}$.

ACKNOWLEDGMENTS

This work was supported by the Research Fund for the Doctoral Program of Higher Education (Grant No.20060504001) and the Foundation for the Author of National Excellent Doctoral Dissertation of China (No. 200767). The authors gratefully acknowledge Xiang-Wen Liu (China University of Geosciences) for his assistance with the TEM analysis.

REFERENCES

De Villiers, J.E. (1983) The manganese deposits of Griqualand West, South Africa; some mineralogic aspects. *Economic Geology*, **78**, 1108−1118.

Dowding, C.E. and Fey, M.V. (2007) Morphological, chemical and mineralogical properties of some manganese-rich oxisols derived from dolomite in Mpumalanga province, South Africa. *Geoderma*, **141**, 23−33.

Feng, Q., Honbu, C., Yanagisawa, K. and Yamasaki, N. (1998) Synthesis of lithiophorite with sandwich layered structure by hydrothermal soft chemical process. *Chemistry Letters*, 757−758.

Feng, Q., Honbu, C., Yanagisawa, K. and Yamasaki, N. (1999) Hydrothermal soft chemical reaction for formation of sandwich layered manganese oxide. *Chemistry of Materials*, **11**, 2444−2450.

Feng, X.H., Liu, F., Tan, W.F., and Liu, X.W. (2004) Synthesis of birnessite from the oxidation of Mn^{2+} by O_2 in alkali medium: Effects of synthesis conditions. *Clays and Clay Minerals*, **52**, 240−250.

Feng, X.H., Zhan, L.M., Tan, W.F., Liu, Fiu, He, J.Z., and Zhu, Y.G. (2007) Adsorption and redox reactions of heavy metals on synthesized Mn oxide minerals. *Environmental Pollution*, **147**, 366−373.

Giovanoli, R., Buhler, H., and Sokolowska, K. (1973) Synthetic lithiophorite: Electron microscopy and X-ray diffraction. *Journal de Microscopie*, **18**, 90−103.

Golden, D.C., Dixon, J.B., and Kanehiro, Y. (1993) The manganese oxide mineral, lithiophorite, in an oxisol from Hawaii. *Australian Journal of Soil Research*, **31**, 51−66.

Kim, J.G., Dixon, J.B., Chusuei, C.C., and Deng, Y. (2002) Oxidation of chromium(III) to (VI) by manganese oxides. *Soil Science Society of America Journal*, **66**, 306−315.

Luo, J., Zhang, Q., Huang, A., Giraldo, O., and Suib, S.L. (1999) Double-aging method for preparation of stabilized Na-buserite and transformations to todorokites incorporated with various metals. *Inorganic Chemistry*, **38**, 6106−6113.

Manceau, A., Marcus, M.A., Tamura, N., Proux, O., Geoffroy, N., and Lanson, B. (2004) Natural speciation of Zn at the micrometer scale in a clayey soil using X-ray fluorescence, absorption and diffraction. *Geochimica et Cosmochimica Acta*, **68**, 2467−2483.

Manceau, A., Tommaseo, C., Rihs, S., Geoffroy, N., Chateigner, D., Schlegel, M., Tisserand, D., Marcus, M.A., Tamura, N., and Chen, Z.S. (2005) Natural speciation of Mn, Ni, and Zn at the micrometer scale in a clayey paddy soil using X-ray fluorescence, adsorption, and diffraction. *Geochimica et Cosmochimica Acta*, **69**, 4007−4034.

McKenzie, R.M. (1971) The synthesis of birnessite, cryptomelane, and some other oxides and hydroxides of manganese. *Mineralogical Magazine*, **38**, 493−503.

McKenzie, R.M. (1989) Manganese oxides and hydroxides. Pp. 439−465 in: *Minerals in Soil Environments* (2nd edition) (J.B. Dixon and S.B. Weed, editors). Book Series **1**, Soil Science Society of America, Madison, Wisconsin, USA.

Ouvrard, S., Donato, P., Simonnot, M.O., Begin, S., Chanbaja, J., Alnot, M., Duval, Y.B., Lhote, F., Barres, O., and Sardin, M. (2005) Natural manganese oxide: Combined analytical approach for solid characterization and arsenic retention. *Geochimica et Cosmochimica Acta*, **69**, 2715−2724.

Post, J.E. (1999) Manganese oxide minerals: Crystal structures and economic and environmental significance. *Proceedings of the National Academy of Science*, **96**, 3447−3454.

Post, J.E. and Appleman, D.E. (1994) Crystal structure refinement of lithiophorite. *American Mineralogist*, **79**, 370−374.

Tan, W.F., Liu, F., Li, Y.H., Hu, H.Q., and Huang, Q.Y. (2006) Elemental composition and geochemical characteristics of iron-manganese nodules in main soils of China. *Pedosphere*, **16**, 72−81.

Uzochukwu, G.A. and Dixon, J.B. (1986) Manganese oxide minerals in nodules of two soils of Texas and Alabama. *Soil Science Society of America Journal*, **50**, 1079−1084.

Vidhana Arachchi, L.P., Tokashiki, Y., and Baba, S. (2004) Mineralogical characteristics and micromorphological observations of brittle/soft Fe/Mn concretions from Okinawan soils. *Clays and Clay Minerals*, **52**, 462−472.

Wadsley, A.D. (1950) Synthesis of some hydrated manganese minerals. *American Mineralogist*, **35**, 485−499.

Yang, D.S. and Wang, M. (2003) Characterization and a fast method for synthesis of sub-micron lithiophorite. *Clays and Clay Minerals*, **51**, 96−101.

(*Received 18 May 2008; revised 18 February 2009; Ms. 0156; A.E. F. Bergaya*)